Eosinophil-derived TGFβ1 controls the new bone formation in chronic rhinosinusitis with nasal polyps*

Sungsin Jo[1,#], Seung Hoon Lee[1,#], Hye-Ryeong Jo[1], Subin Weon[1], Chanhyeok Jeon[1], Min Kyu Park[2], Tae-Hwan Kim[1,3,†], Seok Hyun Cho[2,†]

[1] Hanyang University Institute for Rheumatology Research (HYIRR), Hanyang University, Seoul, Republic of Korea

[2] Department of Otorhinolaryngology-Head and Neck Surgery, Hanyang University College of Medicine, Seoul, Republic of Korea

[3] Department of Rheumatology, Hanyang University Hospital for Rheumatic Diseases, Seoul, Republic of Korea

Rhinology 61: 4, 338 - 347, 2023

https://doi.org/10.4193/Rhin22.439

***Received for publication:**

November 14, 2022

Accepted: April 10, 2023

[#] Contributed equally as first author

[†] Contributed equally as senior author

Abstract

Background: Chronic rhinosinusitis with nasal polyps (CRSwNP) is characterized by chronic eosinophilic inflammation and new bone formation (NBF). These processes may be associated with each other in the pathogenesis and influence the severity and prognosis of the disease. However, it is still unclear how eosinophilic inflammation is involved in the NBF.

Methodology: Sinus bone cells were isolated from ethmoid bone tissues of patients with CRSwNP and controls. Transforming growth factor beta 1 (TGFβ1) and alkaline phosphatase (ALP) expression in sinus bone cells was determined using quantitative RT–PCR, immunoblotting, and immunohistochemistry. The co-localization of TGFβ1 with eosinophils was assessed by immunofluorescence staining. Sinus bone cells were co-cultured with eosinophils (Eol-1 cell line), which were differentiated with butyrate, to measure the osteoblast differentiation activity of sinus bone cells.

Results: TGFβ1 expression was increased in sinus bone tissues and correlated with CT scores in CRSwNP. TGFβ1 was also increased in the submucosa of CRSwNP and co-localized predominantly with eosinophils compared with neutrophils Differentiated Eol-1 cells-derived TGFβ1 increased ALP expression in sinus bone cells. Treatment with a TGFβ1 inhibitor attenuated TGFβ1-induced ALP expression and staining in sinus bone cells of CRSwNP, leading to loss of bone formation.

Conclusions: Eosinophil-derived TGFβ1 was enriched in the submucosa of CRSwNP, which induced ALP expression in sinus bone cells and NBF. Therefore, eosinophil-derived TGFβ1 may mediate aberrant bone remodeling in CRSwNP.

Key words: chronic eosinophilic inflammation, chronic rhinosinusitis with nasal polyps, eosinophil-derived TGFβ1, new bone formation

Introduction

Chronic rhinosinusitis (CRS) is a chronic inflammatory disease of the paranasal sinuses linked to heterogeneous systemic and local factors. In particular, chronic rhinosinusitis with nasal polys (CRSwNP) is characterized by eosinophilic infiltration and new bone formation (NBF), leading to olfactory dysfunction, disability, and refractory CRS [(1-3)]. Growing evidence indicates that eosinophilic infiltration and T helper 2 (Th2)-type inflammation (elevated local expression of eosinophilic cationic protein [ECP], eotaxin, and immunoglobulin E) are strongly associated with the sinus bone thickening, osteitis, increased osteoblast activity, and NBF of CRSwNP [(4-8)]. However, the underlying molecular mechanisms of how eosinophilic mucosal inflammation leads to NBF in CRSwNP remain unclear.

Transforming growth factor-beta (TGFβ) is a multifunctional cytokine produced by a variety of cells in the event of an inflammatory situation. Of these, TGFβ1 is known to be an important regulator involved in the abnormal bone remodeling proces-

ses of bone-related disorders [9,10]. TGFβ1 also is known to be strongly expressed in eosinophils and to induce epithelial-mesenchymal transition (EMT) [11-14]. Moreover, detection of eosinophil-derived TGFβ1 in humans and mice and elevation of TGFB1 expression in the submucosa of human CRS have been reported [15-17]. Previous studies have shown elevated expression of TGFβ1 in CRS, but results were inconsistent and different depending on CRS endotypes. Bachert et al. showed that TGFβ1 levels were higher in CRSsNP than in CRSwNP [18,19]. In contrast, TGFβ1 expression was elevated in osteitis of CRSwNP compared to healthy controls and CRSsNP [20,21]. Various functions of TGFβ1 and heterogeneous CRS endotypes of Th1, Th2, Th17, and mixed inflammation may be an obstacle to understanding the relationship between causal TGFβ1 and resulting NBF in CRS.

This study investigated the underlying basis of aberrant TGFβ1 expression in eosinophilic inflammation and NBF in CRSwNP. We aimed to study the expression level of TGFβ1 in the mucosal and bone tissues of CRSwNP to localise TGFβ1 expression in inflammatory cells of eosinophils, neutrophils, and macrophages. In addition, we used a co-culture system to measure the TGFβ1-secreting ability of differentiated Eol-1 cells, which may induce elevated alkaline phosphatase (ALP) expression in sinus bone cells of CRSwNP, leading to bone mineralisation.

Materials and methods

Study population

This study was approved by the Institutional Review Board of Hanyang University Hospital, and written informed consent was obtained from all the participants (No. 2021-09-006). The participant characteristics are summarized in Table 1.

From April to August 2022, 22 patients with CRSwNP (n=22) who underwent endoscopic sinus surgery (ESS) according to European Position Paper on Rhinosinusitis and Nasal Polyps (EPOS) guidelines were enrolled [22]. The seven controls were cases of endoscopic pituitary surgery (n=7) and cerebrospinal fluid leak (n=1). Clinical data, including demographic information, nasal symptoms, and medical and surgical histories, were recorded. All subjects underwent nasal endoscopy, computed tomography (CT), serological tests (total IgE and complete blood count), and skin prick tests to determine their sensitivity to common inhaled allergens. The severity of the CRSwNP was evaluated using CT scores. Exclusion criteria were CRS without nasal polyposis, fungal sinusitis, mucocoele, and paranasal sinus tumours. To define the presence of NBF, we used the following criteria: increased bone density (Hounsfield unit ≥ 400) on preoperative CT scans and identification of hard ethmoid bone during ESS with a navigation system [23].

Isolation of human sinus bone cells and assessment of osteoblasts differentiation

Table 1. Clinical characteristics of control and CRSwNP.

	Control (n=7)	CRSwNP (n=22)	P value
Sex (M:F)	5:2	16:6	0.647
Age (years)	42.1 ± 17.36	53.0 ± 15.6	0.173
Smoking (%)	28.6	27.2	0.647
Allergy (%)	57.1	36.4	0.295
Asthma (%)	0	22.7	0.222
Total IgE (IU/mL)	103.1 ± 86.9	183.7± 200.2	0.148
Serum eosinophil (%)	3.0 ± 1.9	5.1 ± 3.8	0.068
CT score	5.8 ± 3.9	12.6 ± 3.8	0.001*
Bone density (HU)	215.2 ± 81.8	616.8 ± 177.4	0.001*

CRSwNP, chronic rhinosinusitis with nasal polyps; IgE, immunoglobulin E; CT, computed tomography; HU, Hounsfield unit. *P < 0.001.

Human sinus bone cells were grown using outgrowth culture methods, as previously reported [24]. Isolated sinus bone cells were maintained in DMEM with 10% FBS and 1% antibiotics in a humidified atmosphere of 5% CO_2. In addition, isolated sinus bone cells cultured for 2–5 passages were used in the experiments and checked for mycoplasma using a PCR-based method (6601, Takara) before the in vitro experiments.

Osteoblasts differentiation was assessed according to matrix maturation and mineralization [25,26]. Matrix maturation of osteoblast differentiation was assessed by alkaline phosphatase (ALP; 85L2, Sigma) staining and ALP activity (K412, Biovision). The matrix mineralization of osteoblast differentiation was assessed by Alizarin red (ARS; A5533, Sigma), hydroxyapatite (HA; PA-1503, Lonza), and von Kossa (VON; 1% silver nitrate solution; S7179, Sigma) staining. After staining, the wells were imaged using a Nikon Eclipse Ti-U microscope (MEA510AA, Nikon). For quantification of ARS staining, stained wells were incubated with 200 µL of 10% acetic acid at 37°C for 2 h; 80 µL aliquots of the extracted solution were to each well of a new 96-well plate and measured at 450 nm in a multi-plate reader (51119000, Thermo Fisher Scientific). To quantify HA staining, stained wells were measured at an excitation wavelength of 492 nm and an emission wavelength of 550 nm using a multi-plate reader. For VON quantification, stained well images were selected and analysed using Image J.

The ethmoid bone tissues were immediately dissected from the overlying mucosa using surgical elevators and forceps. The isolated mucosal tissues were placed in 1 mL of TriZOL solution were stored at −20°C. Collected mucosal tissues were homogenised, and total RNA was extracted following standard RNA extraction protocol. Complementary DNA (cDNA) was generated using RevertAid First Strand cDNA Synthesis Kit (K1622, ThermoFisher Scientific). Quantitative PCR (qPCR) was performed on a CFX96

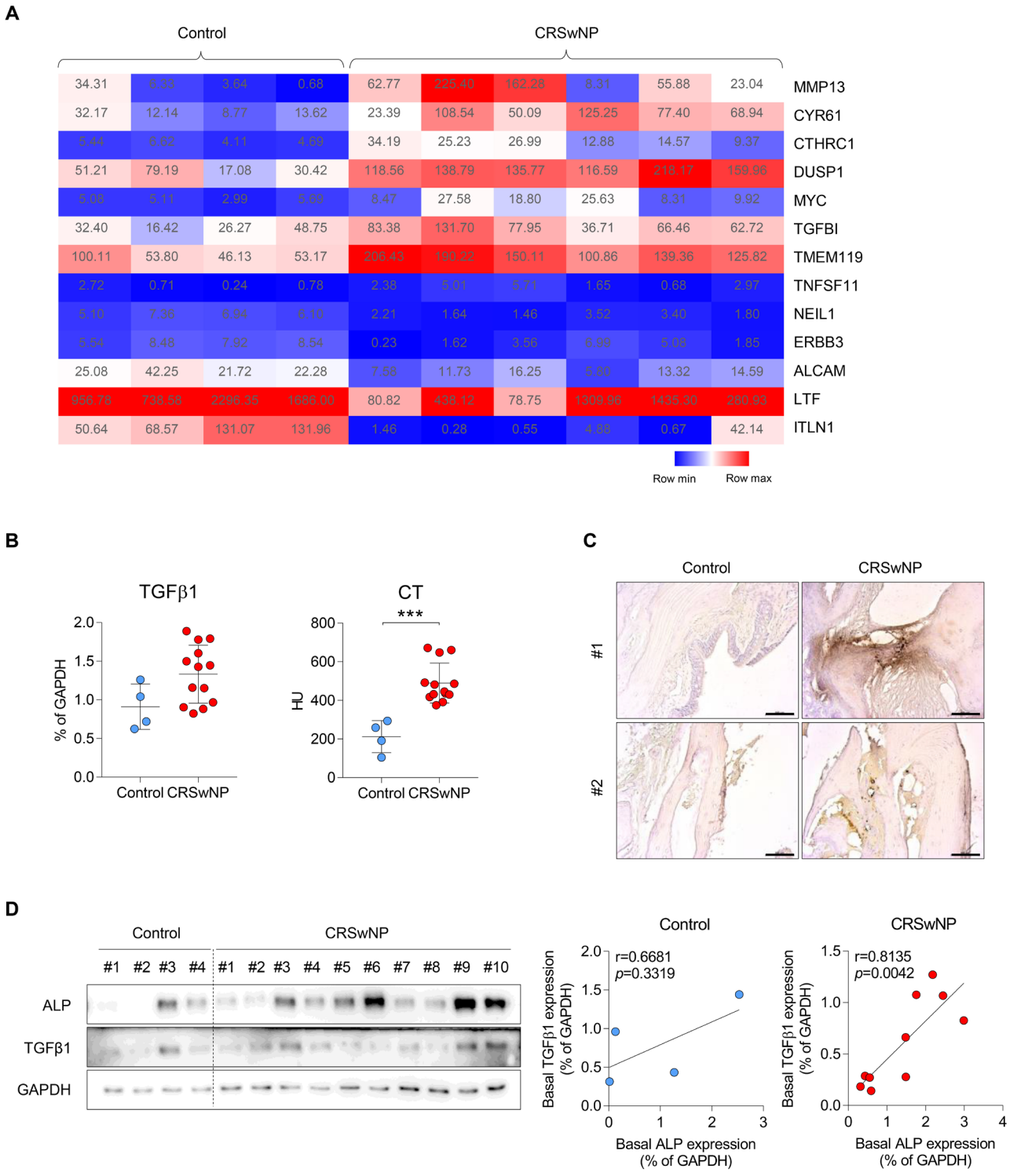

Figure 1. TGFB1 was highly expressed and associated with ALP in ethmoid bone tissues of CRSwNP. (A) Osteoblast-related genes were scanned by RNA-sequencing and the heatmap shows differentially expressed genes associated with osteoblasts in CRSwNP (Control, n=4 and CRSwNP, n=6). (B) TGFB1 mRNA expression and Lund–Mackay CT scores were shown in both control and CRSwNP groups (control, n=4 and CRSwNP, n=12). (C) Both control and CRSwNP ethmoid bone tissues underwent immunohistochemical tests for TGFβ1. Representative images are shown (Control, n=2 and CRSwNP, n=7). Scale bar: 100 μm. (D) Immunoblotting was performed for ALP and TGFB1. Protein intensity was quantified by ImageJ software. The normalised band intensity of each target was adjusted to GAPDH as a loading control. Correlation between ALP and TGFβ1 protein levels of each control and CRSwNP patient group (Control, n=4 and CRSwNP, n=10). Data are expressed as the means ± SEM. *p<0.05, ***p<0.001, Mann–Whiney U test.

Table 2. Human oligonucleotide sequences for qPCR and RT-PCR.

Gene	5' ------ Forward ------ 3'	5'------ Reverse ------ 3'
GAPDH (qPCR)	GTAACCCGTTGAACCCCATTC	CCATCCAATCGGTAGTAGCG
GAPDH (RT-PCR)	GTCAGTGGTGGACCTGACCT	AGGGGTCTACATGGCAACTG
TGFB1 (qPCR)	CGACTCGCCAGAGTGGTTAT	AGTGAACCCGTTGATGTCCA
ALP (RT-PCR)	ACGAGCTGAACAGGAACAACGT	CACCAGCAAGAAGAAGCCTTTG
ECP (qPCR)	CCAGACCCCCACAGTTTACG	GTTCTGTTATGAGGGCAGCG
TPSAB1 (qPCR)	GGCCCATACTGGATGCACTT	GTAGAACTGTGGGTGCACGA
CCL26 (qPCR)	ATACAGCCACAAGCCCCTTC	TGGGTACAGACTTTCTTGCCTC
EPX (qPCR)	CCCATGGACCTCCTGTCCTA	CCGCTGGGGTTGTAACTTCT
ARG1 (qPCR)	ACTTAAAGAACAAGAGTGTGATGTG	ATTGCCAAACTGTGGTCTCC
ELANE (qPCR)	ATTGCGCCCAACTTCGTCAT	AAGTTTACGGGGTCGTAGCC

GAPDH, glyceraldehyde 3-phosphate dehydrogenase; ALP, alkaline phosphatase; TGFB1, transforming growth factor beta 1; ECP, eosinophil cationic protein, TPSAB1, tryptase alpha/beta 1; CCL26, C-C motif chemokine ligand 26; EPX, eosinophil peroxidase; ARG1, arginase 1; ELANE, elastase, neutrophil expressed.

real-time thermocycler (Bio-Rad Laboratories, Hercules, CA, USA) using iQ SYBR Green Supermix (170-8882AP, Bio-Rad) according to the manufacturer's protocol. The target gene expression was normalised for all samples to that of human GAPDH. The oligonucleotide primer sequences are listed in Table 2.

Immunohistochemistry (IHC)

IHC procedures were previously reported [24,25,27]. Ethmoid bone tissues were fixed with 10% formalin for 3 days, decalcified with 10% formic acid for one week, and embedded in paraffin. The paraffin blocks were cut into 5–7 mm-thick sections. Briefly, tissue slides were de-paraffinised, dehydrated, incubated with Antigen Retrieval Kit (VB-6009, VitroVivo Biotech), permeabilised with 0.3% Triton X-100 in 1X TBS-T, and endogenous peroxidase was eliminated with BLOXALL (SP-6000, Vector Lab). They were then incubated overnight at 4°C with the appropriate primary antibodies in antibody diluent (S3022, DAKO). The slides were incubated with ABC kit components (PK-6102, Vector Lab), DAB substrate kit (sk4100, Vector Lab), counterstained with haematoxylin (1.05174.0500, Merck), and mounted with a permanent mounting medium (H-5000, Vector Lab). Images were collected with a Nikon Eclipse Ti-U microscope to visualize stained cells. Five fields for each sample were randomly acquired at 200× magnification.

Co-culture using transwells

Sinus bone cells (1×10^5 cells/well) were cultured in the lower chamber of 12-well transwells (0.4 µm pose size; 3401, Coring). The next day, Eol-1 cells (6×10^5 cells/well) were placed in the upper chamber and exposed to the vehicle or 100 µM butyrate. Transwell cultures were incubated and allowed to migrate to soluble factors for two days. Stimulated Eol-1 cells were harvested from the upper chamber RNA expression analysis. In addition, sinus bone cells in the lower chamber were stained with ALP.

Immunofluorescence (IF)

Sinus bone tissues were fixed in 10% formalin for one week, incubated with 10% formic acid for one week, and embedded in paraffin. Tissue slides (5 µm-thick) were baked at 65°C for 30 min, and the paraffin was removed by two washes (5 min each) with Neo-Clear (1.09843.5000, Merck), followed by dehydration by passage through a graded series of ethanol solutions (100% to 50% ethanol). For permeabilisation, slides were incubated for 10 min with TBS-T (0.3% Triton X-100) and blocked with BLOXALL (SP-6000, Vector Lab) for an hour at room temperature. They were then incubated with proteoglycan 2 (PRG2) (ab14462, Abcam), a specific marker for eosinophils, and TGFβ1 (#8455, Cell Signaling Technology) primary antibodies in an antibody diluent (S3022, Dako) for an hour at room temperature. Antibody binding was visualised using Alexa Fluor 488-conjugated goat anti-mouse antibody (A-11001, Invitrogen) and Cy3-conjugated anti-rabbit antibody (111-165-144, Jackson Immunoresearch). Finally, to remove non-specific signals, the slides were stained by an Autofluorescence Quenching kit (SP-8400, Vector Lab). Immunofluorescence images were acquired by confocal microscopy (Leica Microsystems, Germany), and high-power field counts were obtained at 200× and 400× magnifications. The number of positive cells in each specimen was counted in five random visual fields without non-specific signals. Average values were determined by two independent observers.

Statistical analysis

Graph-Pad Prism 7.0 was used to produce publication-quality images and statistical analysis. Statistical analysis was performed

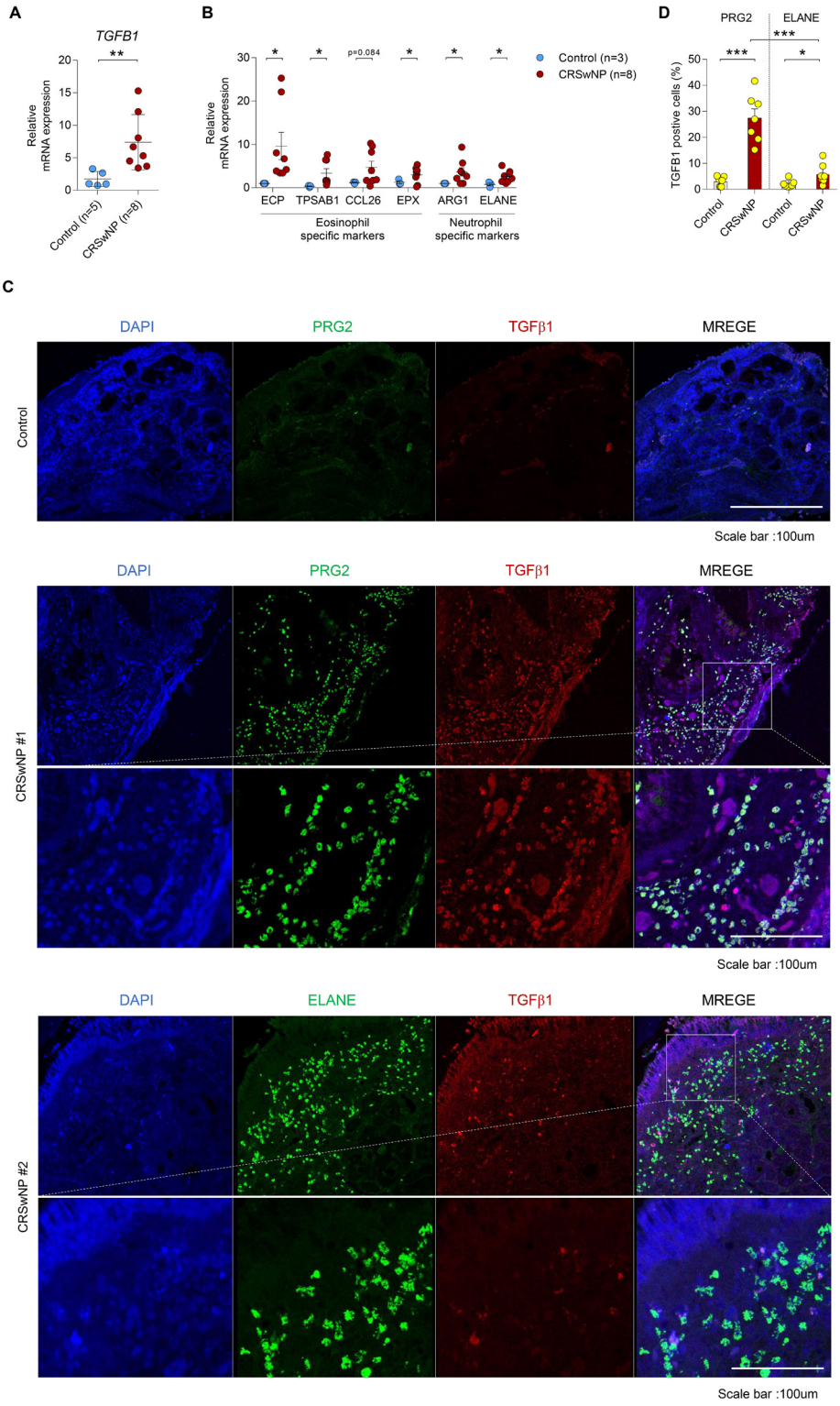

Figure 2. TGFβ1 positive eosinophils were predominant in the submucosa of CRSwNP. Submucosal tissues were harvested from both control and CRSwNP tissues and analysed by RT-qPCR for (A) TGFB1 expression and (B) eosinophil-specific markers; ribonucleases A family member 3 (ECP), Tryptase alpha/beta 1 (TPSAB1), C-C motif chemokine ligand 26 (CCL26), and eosinophil peroxidase (EPX), and neutrophil-specific markers arginase 1 (ARG1) and elastase (ELANE) (Control, n=5 and CRSwNP, n=8). (C) Co-localisation of proteoglycan 2 (PRG2; eosinophil-specific marker, green) or elastase (ELANE; neutrophil-specific marker; green) in TGFβ1 (red) was performed by immunofluorescence in mucosal tissues of both groups. Cell nuclei were counterstained by DAPI (blue, 4'6-diamino-2-phenylindole). Representative images are displayed (control, n=3 and CRSwNP, n=5). (D) Quantification of figure 2C. Images were counted and calculated in 5 different areas. Data are expressed as the means ± SEM. *p<0.05, **p<0.01, ***p<0.001, Mann–Whiney U test. Scale bar: 100 μm.

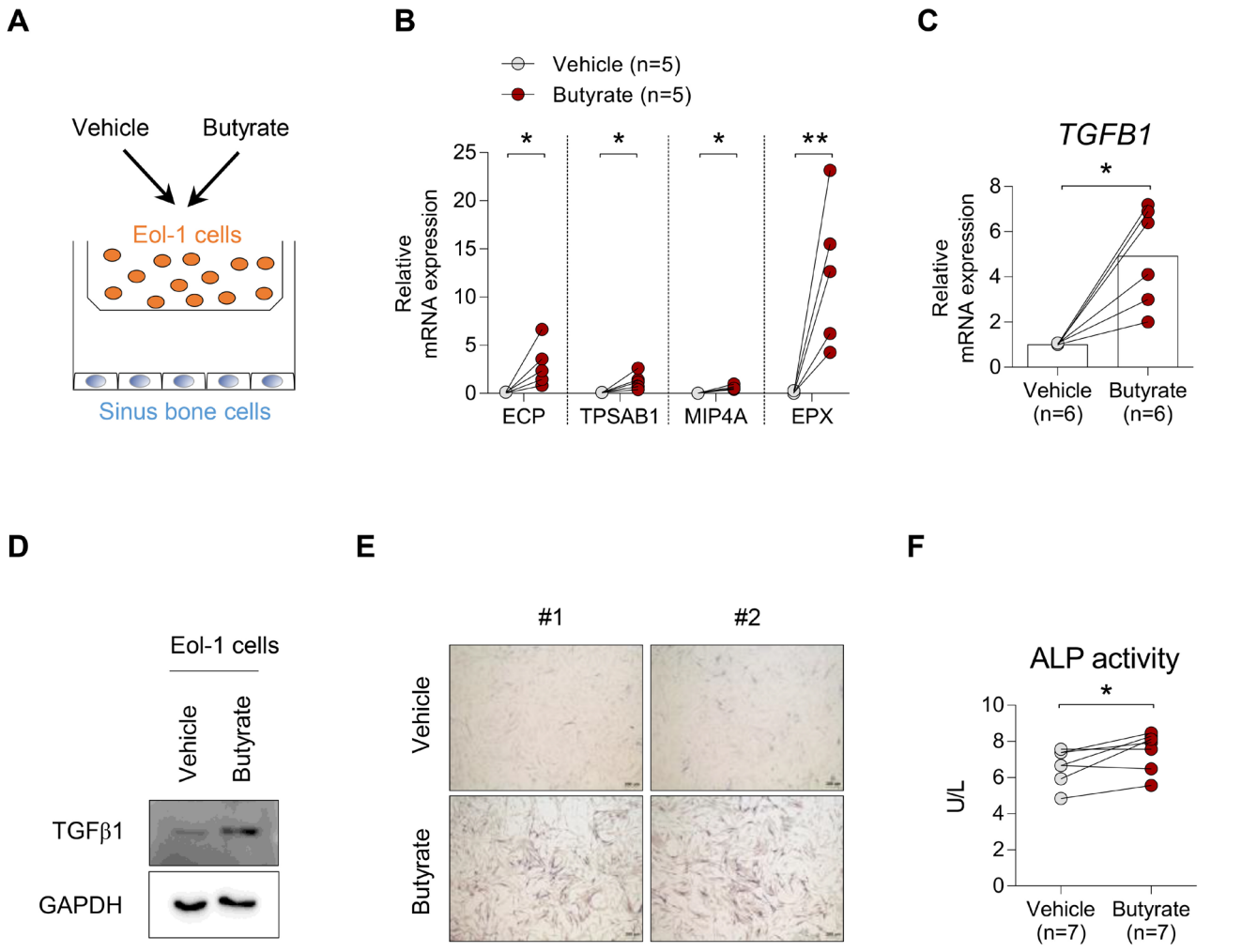

Figure 3. Differentiated Eol-1 cells derived TGFβ1 induced the increased ALP expression in sinus bone cells of CRSwNP. (A) Schematic diagram. The human sinus bone cells of CRSwNP and Eol-1 cells were seeded in the lower and upper chambers, respectively. Eol-1 cells in the upper chamber were treated with vehicle or butyrate for 2 days, harvested, and subjected to (B) RT-qPCR for eosinophil-specific markers, (C) RT-qPCR for TGFB1 expression, and (D) immunoblotting for TGFβ1 expression (n=6 for each group). Sinus bone cells in the lower chamber were stained by (E) ALP staining and (F) ALP activity (n=6 for each group). Data are expressed as the means ± SEM. *p<0.05, **p<0.01, Mann–Whiney U test. Scale bar: 200 μm.

using the Mann–Whitney test with unpaired tests. The values are shown as the mean ± standard error (SEM) from a minimum of three independent experiments. The asterisks represent the level of statistical significance (*P < 0.05, **P < 0.01, ***P < 0.001).

Results

TGFβ1 was increased and positively associated with ALP expression in ethmoid bone tissues of CRSwNP

We previously identified 255 significantly differentially expressed genes (DEG) (fold change > 2 and false discovery rate (FDR) <0.05): 134 genes were upregulated and 91 genes were downregulated in CRSwNP [24]. Among them, specific genes related to osteoblastic and osteoclastic activities are shown in Figure 1A and Figure S1. Here, we confirmed that TGFβ1 expression was increased in the ethmoid bone of CRSwNP compared to that in control using RT-qPCR. Patients with CRSwNP had increased CT scores compared to controls, which showed a positive correlation with TGFβ1 levels of ethmoid bone (r=0.5454, p=0.023, Figure 1B). Immunohistochemistry also showed enriched TGFβ1 expression in the ethmoid bone of CRSwNP (Figure 1C). Immunoblotting revealed that TGFβ1 protein expression was significantly increased in the ethmoid bone of CRSwNP compared with controls, which showed a significant positive correlation with ALP protein levels in CRSwNP (r=0.8135, p=0.0042, Figure 1D). Overall, we found that TGFβ1 was significantly elevated in the ethmoid bone tissues of CRSwNP.

TGFβ1 positive eosinophils were predominant in the submucosa of CRSwNP

Next, we analysed the differential expression of eosinophilic and

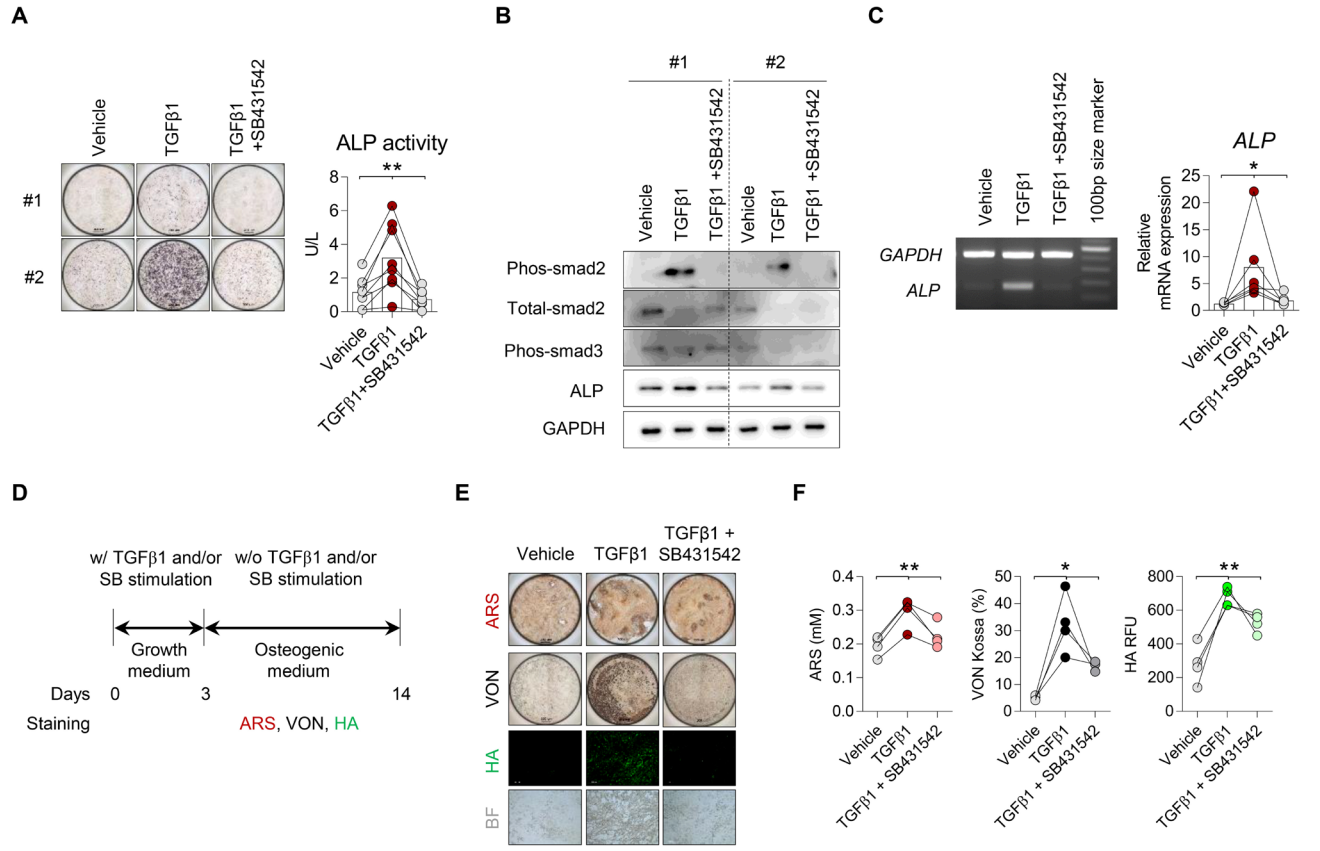

Figure 4. Transient TGFβ1 exposure in sinus bone cells exhibited the promoted bone mineralization in CRSwNP. Sinus bone cells of CRSwNP were treated with vehicle, TGFβ1 alone, and TGFβ1+SB431542 for 2 days and harvested to analyse by (A) ALP staining (left panel) and ALP activity (right panel), (B) immunoblotting, (C) RT-PCR (left panel) and RT-qPCR (right panel). (D) Schematic diagram. Sinus bone cells were pre-treated with exogenous TGFβ1 (10 ng/mL) for 3 days, washed out of TGF1 medium, and incubated with osteogenic differentiation medium for 14 days. At 14 days, differentiated cells were subjected to bone mineralisation-related assay by (E) ARS (upper), VON (central), and HA staining (lower) and (F) its quantification data. Representative images are shown. Data are expressed as the means ± SEM. *p<0.05, **p<0.01, one-way ANOVA with Bonferroni's post-hoc test. Scale bar: 200 μm.

neutrophilic markers in the collected submucosa of patients with CRSwNP. The transcript levels of both eosinophil- and neutrophil-specific markers were significantly higher in the submucosa of patients with CRSwNP than in control (Figure 2A). In addition, TGFβ1 was also highly expressed in the submucosa of CRSwNP (Figure 2B).

Furthermore, we performed immunofluorescence staining to identify the cellular source of TGFβ1 in the submucosa of CRSwNP. As shown in Figure 2C, both eosinophils (PRG2) and neutrophils (ELANE) were enriched in the submucosa of CRSwNP compared with the control. Interestingly, TGFβ1 in CRSwNP was more highly co-expressed in PRG2+ cells than in ELANE+ cells (Figure 2C). Both PRG2+ and ELANE+ cells in CRSwNP were highly co-expressed with TGFβ1, but PRG2+ TGFβ1+ cells were significantly abundant compared to ELANE+ TGFβ1+ cells (Figure 2D). Again, we compared the co-localisation of TGFβ1 with three cell types (eosinophil, neutrophil, and macrophages) in the serial section of a CRSwNP sample; TGFβ1 was predominantly co-localised in PRG2 protein in CRSwNP, but not in ELANE and CD68 (Figure S2). Collectively, we found that co-localisation of TGFβ1 with eosinophils was predominant in the submucosa of CRSwNP.

TGFβ1 secreted by differentiated Eol-1 cells induced the increased ALP expression in sinus bone cells of CRSwNP

To mimic the eosinophilic conditions in the ethmoid sinus of CRSwNP, we co-cultured sinus bone cells (lower chamber) and Eol-1 cells (upper chamber) in the presence of vehicle or butyrate for 48 h (Figure 3A). Differentiation markers of eosinophils were confirmed by RT-qPCR (Figure 3B). Butyrate statistically induced TGFβ1 mRNA and protein expressions in differentiated Eol-1 cells (Figures 3C and 3D). In sinus bone cells co-cultured with differentiated Eol-1 cells, ALP staining and activity significantly increased in the butyrate-treated group (Figures 3E and

3F). Additionally, exogenous TGFβ1 treatment in sinus bone cells resulted in upregulated ALP expression with mRNA and protein levels accompanied by phos-smad 2 protein and downregulated OPG expression (Figures S3A and S3B). However, there were no statistical differences in OPN, RUNX2, or RANKL expression in the TGFβ1-treated group. Taken together, TGFβ1 by differentiated Eol-1 cells induced increased ALP expression in the sinus bone cells of CRSwNP.

Sinus bone cells treated with TGFβ1 exhibited the promoted bone mineralization in CRSwNP

To determine whether TGFβ1 affects osteoblast differentiation of sinus bone cells, we treated sinus bone cells with exogenous TGFβ1 for 3 days and observed TGFβ1-induced matrix mineralisation and maturation by ALP and collagen staining. Consistent with the above findings, transient TGFβ1 treatment dramatically induced ALP expression, whereas co-treatment with a TGFβ1 inhibitor (SB431542) reduced its mediated ALP activity and staining (Figure 4A). Transient TGFβ1 treatment upregulated ALP mRNA and protein levels accompanied by phos-smad2 protein induction, but SB431542 treatment inhibited these effects (Figures 4B and 4C). Next, we experimentally designed that whether the induction of ALP by TGFβ1 transient treatment affect bone formation of sinus bone cells, as shown in the Figure 4D. As expected, transient TGFβ1 treatment enhanced matrix mineralisation in sinus bone cells, but SB431542 treatment suppressed those effects (Figures 4E and 4F). Taken together, these results suggest that transient TGFβ1 exposure promoted bone formation in the sinus bone cells of CRSwNP.

Discussion

Here we revealed that eosinophils were markedly enriched in the mucosa of patients with CRSwNP and co-localised with TGFβ1 protein. Furthermore, differentiated eosinophils induced TGFβ1 expression, which increased the ALP expression of sinus bone cells, leading to NBF of CRSwNP. These changes could be reduced by treatment with a TGFβ1 inhibitor.

A recent understanding of CRS phenotypes and endotypes allows for patient-specific treatment, especially in recurrent or recalcitrant cases [28-30]. As shown in Figures 2B and C, both eosinophils and neutrophils were found in CRSwNP, but major effector cells differ depending on the underlying types of Th inflammation (type 2 versus non-type 2). In eosinophilic CRSwNP, TGFβ1 was markedly stained in eosinophils compared to neutrophils or macrophages (Figure S2). Although neutrophilic CRSwNP showed a statistically increased staining of TGFβ1 compared to the control group, TGFβ1 co-localisation was more prominent in the eosinophilic conditions of CRSwNP (Figure 2D). These findings provide more specific targets for therapeutic intervention and a different strategy for patients with eosinophilic or neutrophilic in CRSwNP.

CRSwNP shows typical features of eosinophilic inflammation and NBF, yet how eosinophils affect bone remodelling and specific target molecules remains largely unknown. In CRS, many studies have described the epithelial-mesenchymal transition (EMT) induction of the nasal epithelium by TGFβ1 and its molecular mechanism [31-34]. Factors such as retinoic acid, vitamin D3, bone morphogenic proteins (BMPs), and WNT molecules are known to induce ALP and, presumably, elevated bone formation and its related signalling pathway activation. Although TGFβ1 induces increased ALP transcript through smad2 protein and bone formation [35], we here revealed that TGFβ1 was strongly co-expressed with eosinophils in the submucosa and affected NBF in CRSwNP.

Bone formation is a sequential and dynamic process and is divided into matrix maturation and mineralization [36]. Indicators and markers that appear at each stage differ; ALP and type 1 collagen for matrix maturation and calcium deposit and hydroxyapatite formation for mineralization are technically represented. We previously demonstrated that eosinophil-derived interferon-gamma (IFN-γ) induces TMEM119 expression in sinus bone cells to drive bone matrix mineralisation in NBF of CRSwNP [24]. Stimulation of IFN-γ is responsible for increased matrix mineralization (ARS, VON, and HA) in the sinus bone cells of CRSwNP but not in matrix maturation (ALP and COL). The effect of stimulation on matrix maturation in sinus bone cells of CRSwNP needs further investigation. In general, ALP gradually increases during the matrix maturation stage of osteoblast differentiation and until mineralization. ALP-positive cells are essential indicators in maintaining bone homeostasis and bone formation [37]. Consistent with previous reports, RNA-sequencing data showed that TGFβ1 was highly expressed in the sinus bone of CRSwNP; our data showed that TGFβ1 expression increased and ALP-positive cells accumulated in sinus bone cells of CRSwNP compared to control tissues (Figure 1D). Moreover, stimulation with TGFβ1 dramatically induced ALP expression in sinus bone cells of CRSwNP. Collectively, our data indicated that the relation between TGFβ1 and ALP in sinus bone cells contributed to the NBF of CRSwNP.

This study had limitations. First, we did not test the effects of other molecules in the TGF-β family (e.g., TGFβ2 and TGFβ3) in sinus bone cells. Second, whether cytokine stimulation can maximise TGFβ1 expression and secretion in differentiated Eo-1 cells by butyrate is questionable. Third, primary eosinophils derived from the submucosa of CRSwNP need further investigation. Finally, because we collected surgical samples only of CRSwNP and studied its pathophysiology, a comparative study between CRSsNP and CRSwNP stills needs to be conducted.

Conclusion

We found that TGFβ1 was strongly co-expressed with eosinophils in CRSwNP. Differentiated eosinophils induce TGFβ1 expression, leading to increased ALP expression in sinus bone cells and bone-forming activity in CRSwNP. Therefore, we provide an important link between eosinophilic infiltration and NBF in CRSwNP.

Authorship contribution

SJ, SL, HJ, CJ, and SW performed the experiments and analysed the data. PMK and SC provided ethmoid bone tissue. SJ, TK, and SC supervised the experimental design, manuscript writing, and editing. All authors have read and approved the final manuscript. We would like to thank Editage (www.editage.co.kr) for English language editing.

Acknowledgement

None.

Conflict of interest

The authors declare that they have no conflict of interest..

Funding

This work was supported by the Basic Science Research Program of the National Research Foundation of Korea (2021R1F1A1049413, 2021M3H4A4079522, 2019R1A2C2004214, 2020R1A2C1102386, and 2021R1A6A1A03038899).

References

1. Schleimer RP. Immunopathogenesis of chronic rhinosinusitis and nasal polyposis. Annu Rev Pathol. 2017;12:331-57.
2. Khalmuratova R, Shin HW. Crosstalk between mucosal inflammation and bone metabolism in chronic rhinosinusitis. Clin Exp Otorhinolaryngol. 2021;14(1):43-9.
3. Kim JY, Lim S, Lim HS, et al. Bone morphogenetic protein-2 as a novel biomarker for refractory chronic rhinosinusitis with nasal polyps. J Allergy Clin Immunol. 2021;148(2):461-72 e13.
4. Snidvongs K, McLachlan R, Sacks R, et al. Correlation of the Kennedy Osteitis Score to clinico-histologic features of chronic rhinosinusitis. Int Forum Allergy Rhinol. 2013;3(5):369-75.
5. Snidvongs K, McLachlan R, Chin D, et al. Osteitic bone: a surrogate marker of eosinophilia in chronic rhinosinusitis. Rhinology. 2012;50(3):299-305.
6. Meng Y, Lou H, Wang C, et al. Predictive significance of computed tomography in eosinophilic chronic rhinosinusitis with nasal polyps. Int Forum Allergy Rhinol. 2016;6(8):812-9.
7. Videler WJ, Georgalas C, Menger DJ, et al. Osteitic bone in recalcitrant chronic rhinosinusitis. Rhinology. 2011;49(2):139-47.
8. Youn Bk, Kim D-K, Kim BH, et al. Local allergic inflammation in chronic rhinosinusitis with nasal polyps could influence on disease severity and olfaction. Rhinology. 2021;28(3):147-52.
9. Wu M, Chen G, Li YP. TGF-beta and BMP signaling in osteoblast, skeletal development, and bone formation, homeostasis and disease. Bone Res. 2016;4:16009.
10. Crane JL, Cao X. Bone marrow mesenchymal stem cells and TGF-beta signaling in bone remodeling. J Clin Invest. 2014;124(2):466-72.
11. Wang QP, Escudier E, Roudot-Thoraval F, et al. Myofibroblast accumulation induced by transforming growth factor-beta is involved in the pathogenesis of nasal polyps. Laryngoscope. 1997;107(7):926-31.
12. Melo RC, Liu L, Xenakis JJ, et al. Eosinophil-derived cytokines in health and disease: unraveling novel mechanisms of selective secretion. Allergy. 2013;68(3):274-84.
13. Kim SJ, Park JH, Lee SA, et al. All-trans retinoic acid regulates TGF-beta1-induced extracellular matrix production via p38, JNK, and NF-kappaB-signaling pathways in nasal polyp-derived fibroblasts. Int Forum Allergy Rhinol. 2020;10(5):636-45.
14. Ohno I, Lea RG, Flanders KC, et al. Eosinophils in chronically inflamed human upper airway tissues express transforming growth factor beta 1 gene (TGF beta 1). J Clin Invest. 1992;89(5):1662-8.
15. Fallegger A, Priola M, Artola-Boran M, et al. TGF-beta production by eosinophils drives the expansion of peripherally induced neuropilin(-) RORgammat(+) regulatory T-cells during bacterial and allergen challenge. Mucosal Immunol. 2022;15(3):504-14.
16. Minshall EM, Leung DY, Martin RJ, et al. Eosinophil-associated TGF-beta1 mRNA expression and airways fibrosis in bronchial asthma. Am J Respir Cell Mol Biol. 1997;17(3):326-33.
17. Balsalobre L, Pezato R, Perez-Novo C, et al. Epithelium and stroma from nasal polyp mucosa exhibits inverse expression of TGF-beta1 as compared with healthy nasal mucosa. J Otolaryngol Head Neck Surg. 2013;42:29.
18. Li X, Meng J, Qiao X, et al. Expression of TGF, matrix metalloproteinases, and tissue inhibitors in Chinese chronic rhinosinusitis. J Allergy Clin Immunol. 2010;125(5):1061-8.
19. Van Bruaene N, Derycke L, Perez-Novo CA, et al. TGF-beta signaling and collagen deposition in chronic rhinosinusitis. J Allergy Clin Immunol. 2009;124(2):253-9, 9 e1-2.
20. Wen W, Zhu S, Ma R, et al. Correlation analysis of TGF-beta1, MMP-9, TIMP-1, IL-1, IL-4, IL-6, IL-17, and TNF-alpha in refractory chronic rhinosinusitis: A retrospective study. Allergol Immunopathol (Madr). 2022;50(4):137-42.
21. Wang M, Ye T, Liang N, et al. Differing roles for TGF-beta/Smad signaling in osteitis in chronic rhinosinusitis with and without nasal polyps. Am J Rhinol Allergy. 2015;29(5):e152-9.
22. Fokkens WJ, Lund VJ, Hopkins C, et al. European Position Paper on Rhinosinusitis and Nasal Polyps 2020. Rhinology. 2020;58(Suppl S29):1-464.
23. Cashman EC, Macmahon PJ, Smyth D. Computed tomography scans of paranasal sinuses before functional endoscopic sinus surgery. World J Radiol. 2011;3(8):199-204.
24. Jo S, Jin BJ, Lee SH, et al. Eosinophil-derived interferon-gamma drives transmembrane protein 119-induced new bone formation in chronic rhinosinusitis with nasal polyps. Int Forum Allergy Rhinol. 2022.
25. Jo S, Won EJ, Kim MJ, et al. STAT3 phosphorylation inhibition for treating inflammation and new bone formation in ankylosing spondylitis. Rheumatology (Oxford). 2021;60(8):3923-35.
26. Jo S, Nam B, Lee YL, et al. The TNF-NF-κB-DKK1 axis promoted bone formation in the enthesis of ankylosing spondylitis. J Rheumatic Dis. 2021;28(4):216-24.
27. Jo S, Lee JS, Nam B, et al. SOX9(+) enthesis cells are associated with spinal ankylosis in ankylosing spondylitis. Osteoarthritis Cartilage. 2022;30(2):280-90.
28. Akdis CA, Bachert C, Cingi C, et al. Endotypes and phenotypes of chronic rhinosinusitis: a PRACTALL document of the European Academy of Allergy and Clinical Immunology and the American Academy of Allergy, Asthma & Immunology. J Allergy Clin Immunol. 2013;131(6):1479-90.
29. Bailey LN, Garcia JAP, Grayson JW. Chronic rhinosinusitis: phenotypes and endotypes. Curr Opin Allergy Clin Immunol. 2021;21(1):24-9.
30. Kim DK, Lim HS, Eun KM, et al. Subepithelial neutrophil infiltration as a predictor of the surgical outcome of chronic rhinosinusitis with nasal polyps. Rhinology. 2021;59(2):173-80.

31. Cho JS, Kang JH, Shin JM, et al. Inhibitory effect of delphinidin on extracellular matrix production via the MAPK/NF-kappaB pathway in nasal polyp-derived fibroblasts. Allergy Asthma Immunol Res. 2015;7(3):276-82.
32. Shin JM, Park JH, Park IH, et al. Pirfenidone inhibits transforming growth factor beta1-induced extracellular matrix production in nasal polyp-derived fibroblasts. Am J Rhinol Allergy. 2015;29(6):408-13.
33. Qin D, Liu P, Zhou H, et al. TIM-4 in macrophages contributes to nasal polyp formation through the TGF-beta1-mediated epithelial to mesenchymal transition in nasal epithelial cells. Front Immunol. 2022;13:941608.
34. Sproson EL, Thomas KM, Lau LC, et al. Common airborne fungi induce species-specific effects on upper airway inflammatory and remodelling responses. Rhinology. 2016;54(1):51-5.
35. Chang HH, Chang MC, Wu IH, et al. Role of ALK5/Smad2/3 and MEK1/ERK Signaling in transforming growth factor beta 1-modulated growth, collagen turnover, and differentiation of stem cells from apical papilla of human tooth. J Endod. 2015;41(8):1272-80.
36. Beck GR, Jr., Zerler B, Moran E. Phosphate is a specific signal for induction of osteopontin gene expression. Proc Natl Acad Sci U S A. 2000;97(15):8352-7.
37. Harris H. The human alkaline phosphatases: what we know and what we don't know. Clin Chim Acta. 1990;186(2):133-50.

Seok Hyun Cho, MD, PhD
Department of Otorhinolaryngology
Head and Neck Surgery
Hanyang University College of Medicine
222-1 Wangsimni-ro
Seongdong-gu
Seoul 04763
Republic of Korea

Tel: 82-2-2290-8583
Fax: 82-2-2290-8588
E-mail: shcho@hanyang.ac.kr

This manuscript contains online supplementary material

SUPPLEMENTARY MATERIAL

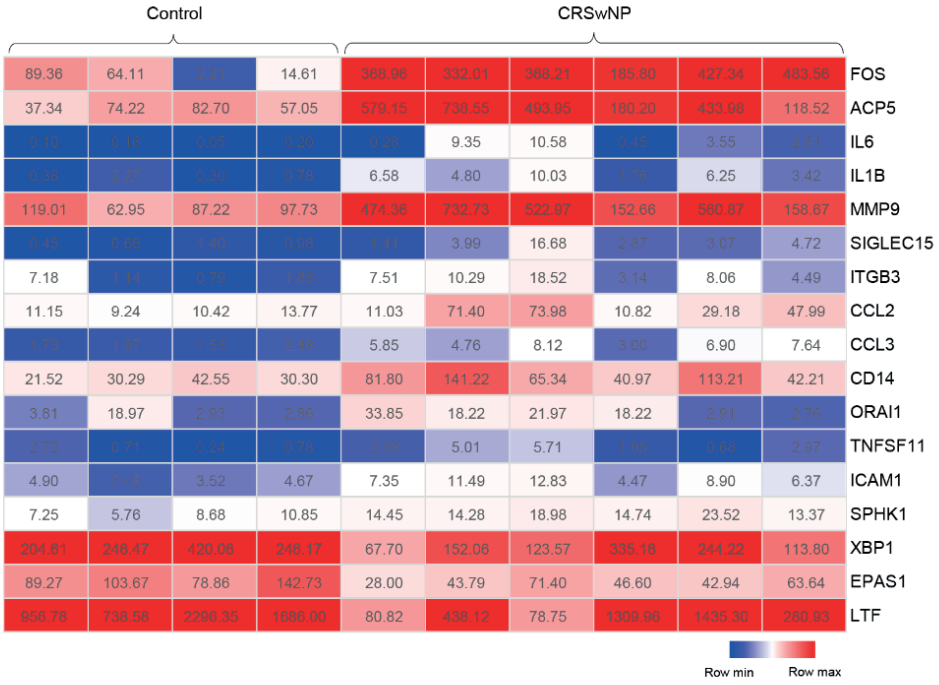

Figure S1. Osteoclast-related genes in RNA-seq data of CRSwNP. Heatmap of osteoclast-related genes were selected and shown.

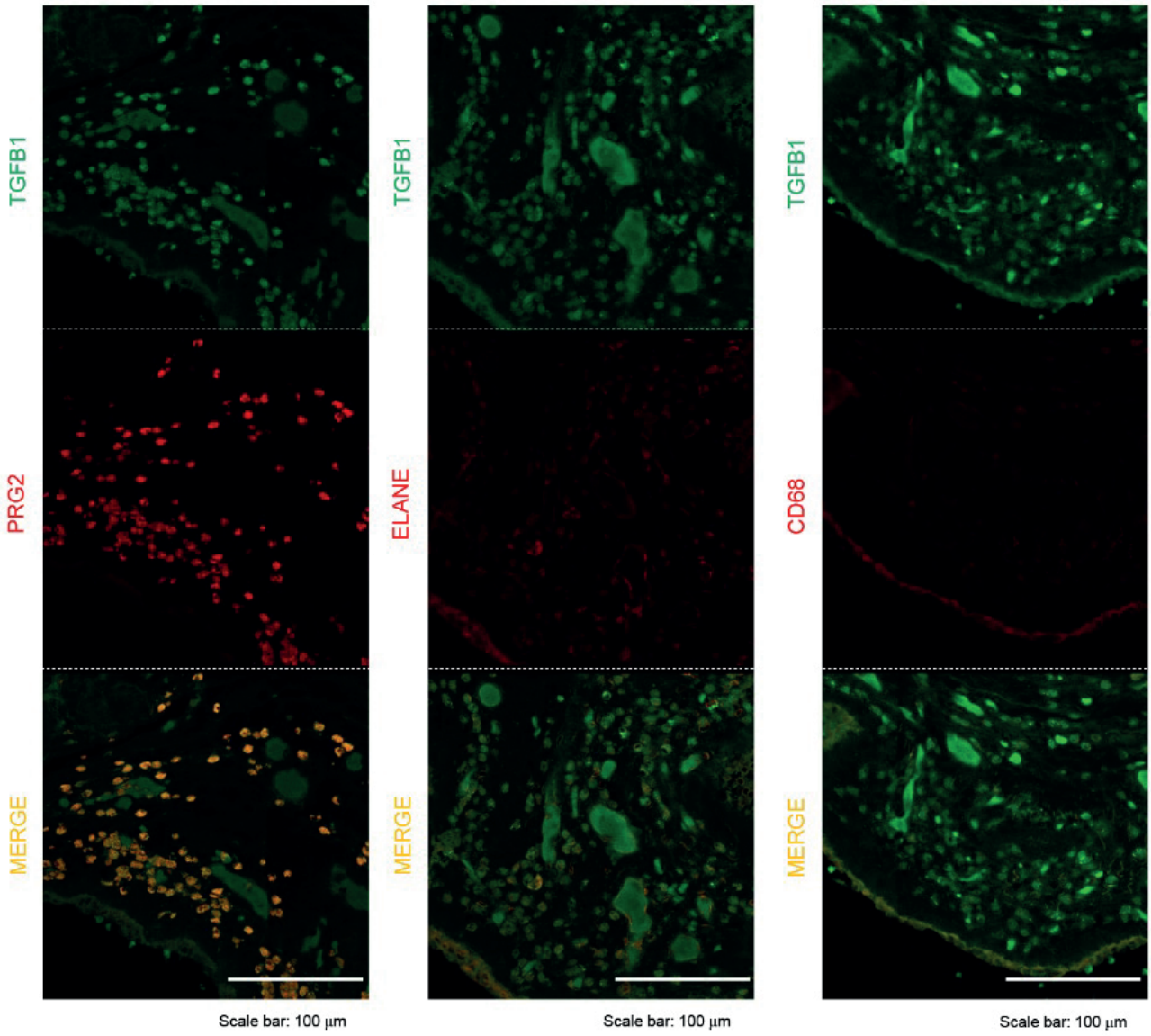

Figure S2. Comparison of TGFB1 with eosinophils, neutrophils, or macrophages in submucosal of CRSwNP. PRG2 (eosinophils), ELANE (neutrophils), or CD68 (macrophages) in presence of TGFB1 were co-immunostained in similar location of submucosal in a patient with CRSwNP. Scale bar: 100 μm.

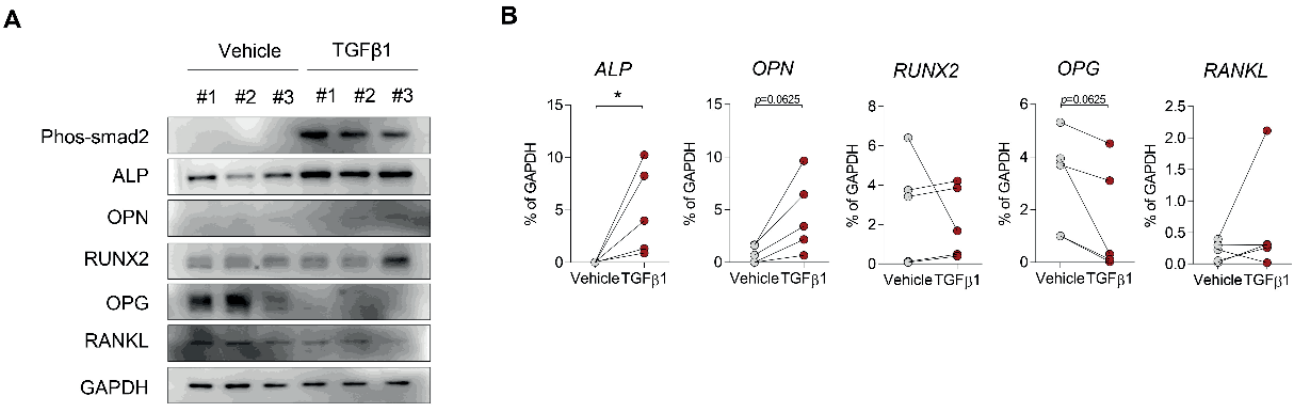

Figure S3. Transient TGFβ1 treatment induced ALP expression by activating phos-smad2 protein. Human sinus bone cells of CRSwNP were treated with exogenous TGFβ1 (25 ng/mL) for a day and analysed by (A) immunoblotting and (B) RT-qPCR (n=5 for each group). Data are expressed as the means ± SEM.